

Solid Freeform Fabrication by Selective Area Laser Deposition

G. -S. Zong, R. Carnes, H. G. Wheat, and H. L. Marcus

*Center for Materials Science & Engineering
The University of Texas at Austin, Austin, TX 78712*

ABSTRACT

Laser chemical vapor deposition is capable of selective area deposition of thin films at high spatial resolution, and in the present work this advantage was used to perform solid freeform fabrication (SFF). The pyrolytic selective area laser deposition of carbon is studied as a function of the scanning speed, the laser power, and the diameter of the focal spot on the substrate, at different pressures of the acetylene precursor in a gas phase SFF system. Carbon rods and rings have been made. SEM and Raman microprobe were used to characterize the deposits.

1. INTRODUCTION

Laser chemical vapor deposition (LCVD) offers a proven technique for single-step local deposition or direct writing of thin films of metals, semiconductors or insulators [1,2]. There are basically two interactions between the laser and the gas/substrate system. The first is a laser induced pyrolytic reaction where the substrate is locally heated and the second is where the gas phase photolytically absorbs the laser energy where the modified gas phase precursor will then be deposited. In pyrolytic LCVD, the deposition rates are high so that three-dimensional structures can be produced. Combining the idea of solid freeform fabrication, which is the integrated approach used to make a component with computer-aided design [3], with selective area laser deposition (SALD), a new process, SFF from gas phase, is defined. SALD has potential of producing parts of novel composite materials at molecular resolution.

In this paper, we present some initial results of SFF from the gas phase.

2. EXPERIMENTAL

The experimental set-up is schematically shown in Fig.1. The TEM₀₀ mode of a pulsed CO₂ ($\lambda=10.6\mu\text{m}$) laser (modulation 5 kHz, maximum output of 25W) was used to locally heat an alumina substrate. To vary its size, the beam was focused by a ZnSe lens with a focal length, f , of 50mm. For accurate adjustment of the laser focus and monitoring the deposition process, a video camera was used. The beam waist $w_0 = 2f\lambda/\pi a = 112.5\mu\text{m}$, where a is the diameter of the beam on the lens of focus length f . The focal depth

is given by $L = 2\pi w_0^2/\lambda = 7.5\text{mm}$. A helium-neon laser beam, running collinearly, assisted in visualizing the path of the CO_2 laser beam. The alumina substrate was 1mm thick with its smooth surface as received. The substrate was cleaned using methanol before put it in the reaction chamber. The reaction chamber, setting on x-y-z mechanical translator, was constructed from a stainless steel cylinder with an outside diameter of 6 inches and a height of 5 inches. A ZnSe window was installed on the top of the chamber to transmit the CO_2 - $10.6\mu\text{m}$ laser beam. The chamber was evacuated initially to 0.1 Torr with a rotary pump,

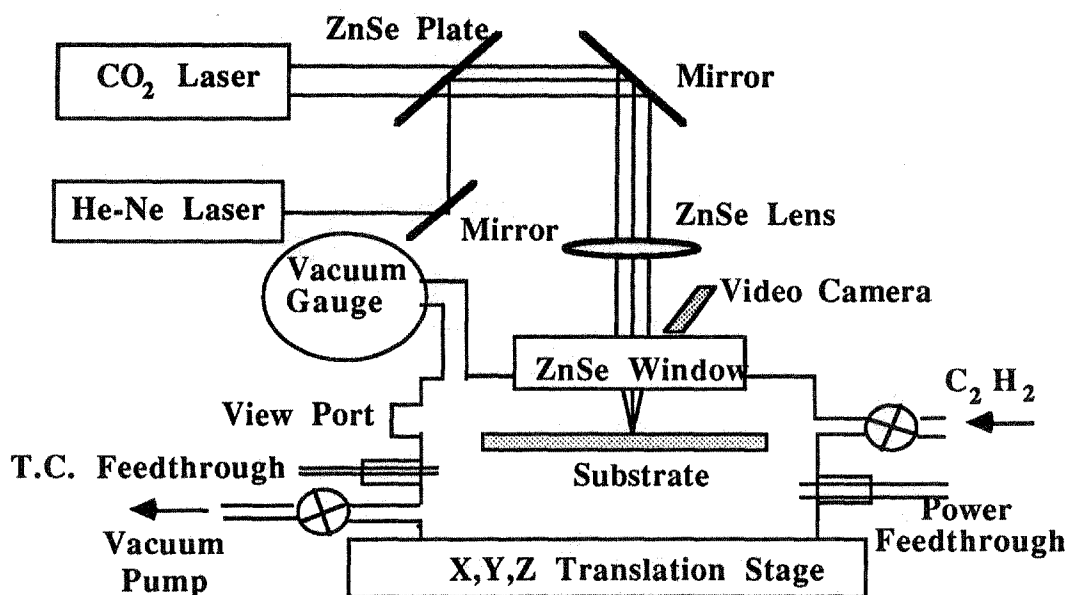


Fig.1 Experimental arrangement used for SFF by SALD

prior to introduction of the source gas. A static fill method over a range of pressures was employed. The source gas used in the experiments reported here was acetylene (C_2H_2 , 99.99% pure).

For safety considerations, the gas supply, laser sources, and reaction chamber were installed and operated under an exhaust hood.

3. RESULTS AND DISCUSSION

3.1 Deposition of rods

The initiation of deposition is readily recognized *in situ* by observing the occurrence on the video screen. When the positions of laser beam and the substrate are both fixed, after the nucleation stage, the growth of a microscopic rod was identified. A typical example of a carbon rod which was grown on an alumina plate is shown in Fig. 2. Two stages of growth can be clearly identified: Near the onset the deposition rate is strongly dependent on the physical and chemical properties of the substrate material and on the thickness of the

deposited material. In the stage of steady growth, which is characterized in Fig. 2 by a constant rod diameter, the deposition rate depends on the laser power, the molecular species, and their concentration (partial pressure), and on the physical properties of the deposit, mainly on its reflectivity and thermal conductivity, but not on the substrate material. Fig. 3 shows the rod diameter decreased when the laser power changed from 10W to 5W, indicating increasing laser power decreases the resolution.

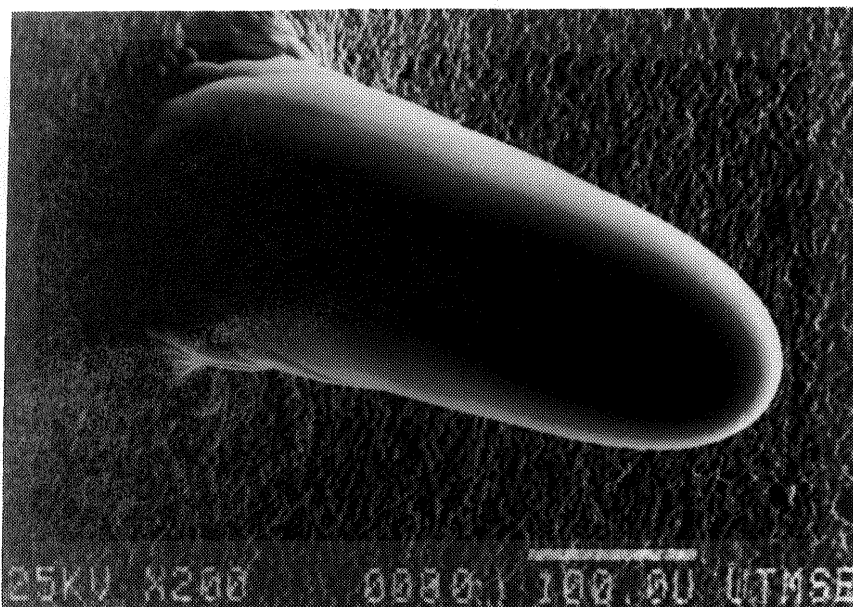


Fig. 2 Carbon rod grown from C_2H_2 ; $p_{C_2H_2}=200$ Torr, $\lambda=10.6\mu m$, $P_{tot}=5$ W

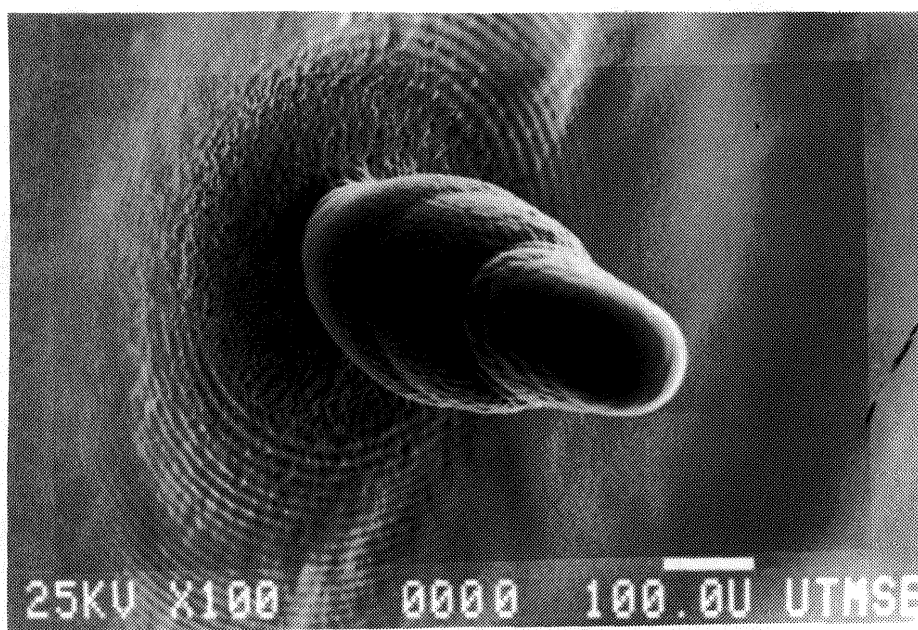


Fig. 3 Carbon rod grown from C_2H_2 ; $p_{C_2H_2}=200$ Torr, $\lambda=10.6\mu m$, $P_{tot}=10$ W, 5W

3.2 Deposition of rings

When the experimental setup of Fig. 1 is operated so that the substrate moves, a requirement for SALD, one can generate material patterns whose shapes depend on the relative motion of the laser beam and the substrate. By multiple scanning, three dimensional parts can be produced. Fig. 4 shows a SEM micrograph of a carbon ring 5mm in diameter, 50 μm in width, and 100 μm in thickness. This ring was grown with $P_{\text{tot}} = 8\text{W}$ of $\lambda = 10.6\mu\text{m}$ CO_2 laser radiation, 2 hours total running time, and a scanning velocity, s , of 42 $\mu\text{m/s}$. The substrate material was alumina. From the data given here, the estimated thickness for each scanning is about 5 μm . A part of the ring in Fig. 4 is shown in Fig. 5. The line width is well defined. Some parts of the ring are irregular, which is probably due to either the nature of the step motor or low scanning speed. This problem will be addressed by using a laser scanning system or improved translation table. A single scan is shown in Fig. 6. The marker indicates where the P_{tot} was changed from 8W to 5W. It is clear that for higher laser power, both the width and the thickness of the line increase.

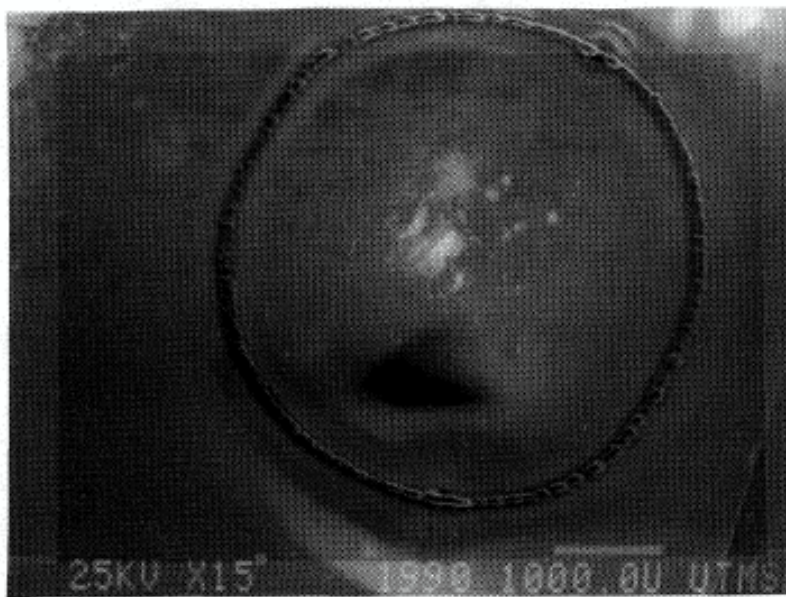


Fig. 4 Carbon ring grown on an alumina substrate,
 $p_{\text{C}_2\text{H}_2} = 200 \text{ Torr}$, $\lambda = 10.6\mu\text{m}$, $P_{\text{tot}} = 8\text{W}$, $s = 42\mu\text{m/s}$.

3.3. Physical properties of deposits

Raman spectroscopy is a fast and sensitive method of determining the bonding state of carbon deposits. The first order phonon mode of cubic diamond is a remarkably invariant feature. The diamond films deposited on hard substrates such as alumina, however, gave Raman bands that were shifted from expected 1332 cm^{-1} in the range of 4~13

wavenumbers, with both positive and negative shifts being observed [4]. These were interpreted as due to local stress induced by mismatch between diamond film and substrate. Raman peaks for graphite have been observed at values from 1500 to 1600 cm^{-1} and the 1350 and 1560 cm^{-1} peaks are typical of diamond-like carbon (DLC) [5].

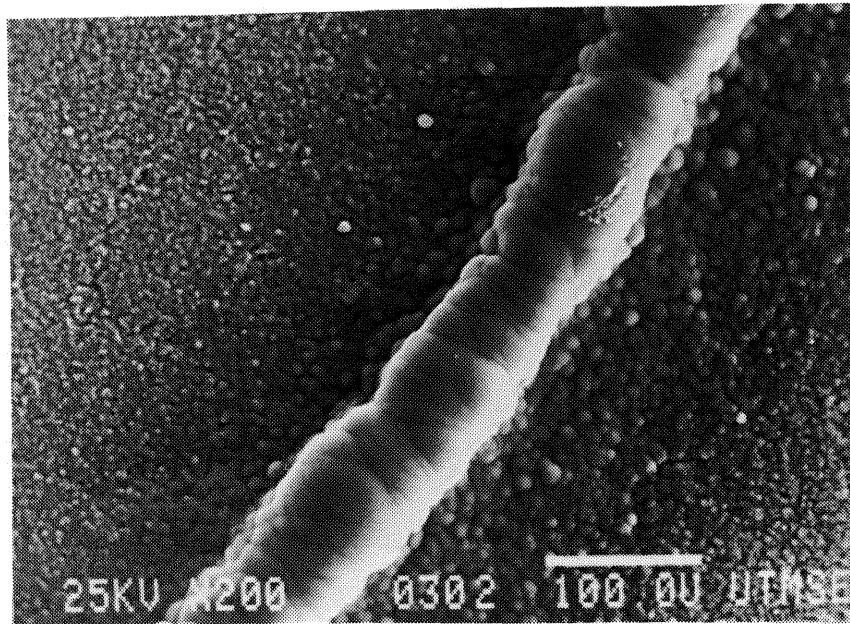


Fig. 5 A part of the carbon ring in Fig. 4

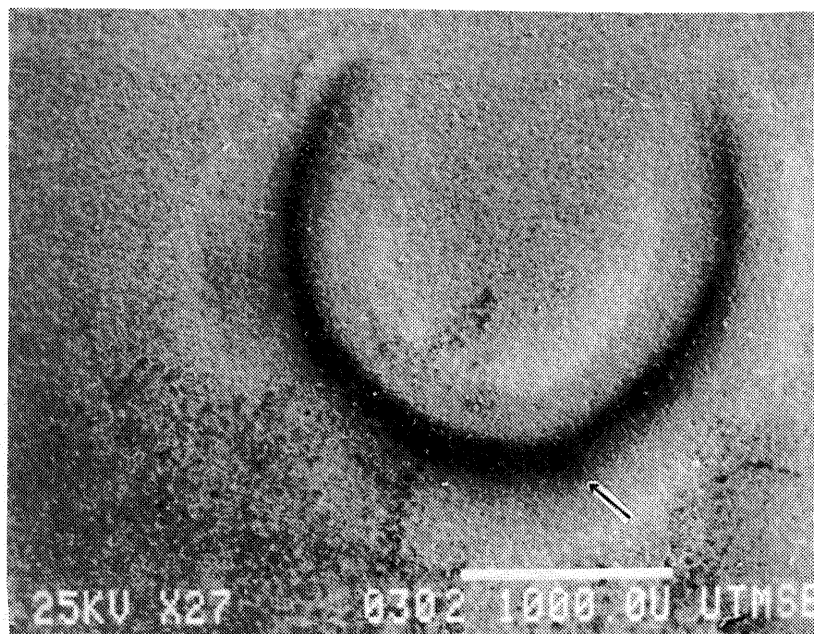


Fig. 6. A single scan carbon deposit on an alumina substrate, $p_{\text{C}_2\text{H}_2}=200$ Torr, $\lambda=10.6\mu\text{m}$, $P_{\text{tot}}=8\text{W}$, 5W , $s=42\mu\text{m/s}$.

The Raman microprobe was used to characterize deposits from the SALD. The Raman spectrum in Fig. 7a shows the presence of diamond and graphite for the deposit in Fig. 3. The expected diamond peak at 1332 cm^{-1} appeared at 1340 cm^{-1} , due to the stress effect, with fine structure. The peak at 1569 cm^{-1} is characteristic of graphite. The Raman analysis of the deposit in Fig. 2 shows the presence of graphite (1584 cm^{-1} peak) and DLC (1348 cm^{-1} peak) (Fig. 7b). By controlling the deposition conditions, such as laser power density, source gas pressure, and substrate temperature, it is possible to get the deposits with different types of carbon.

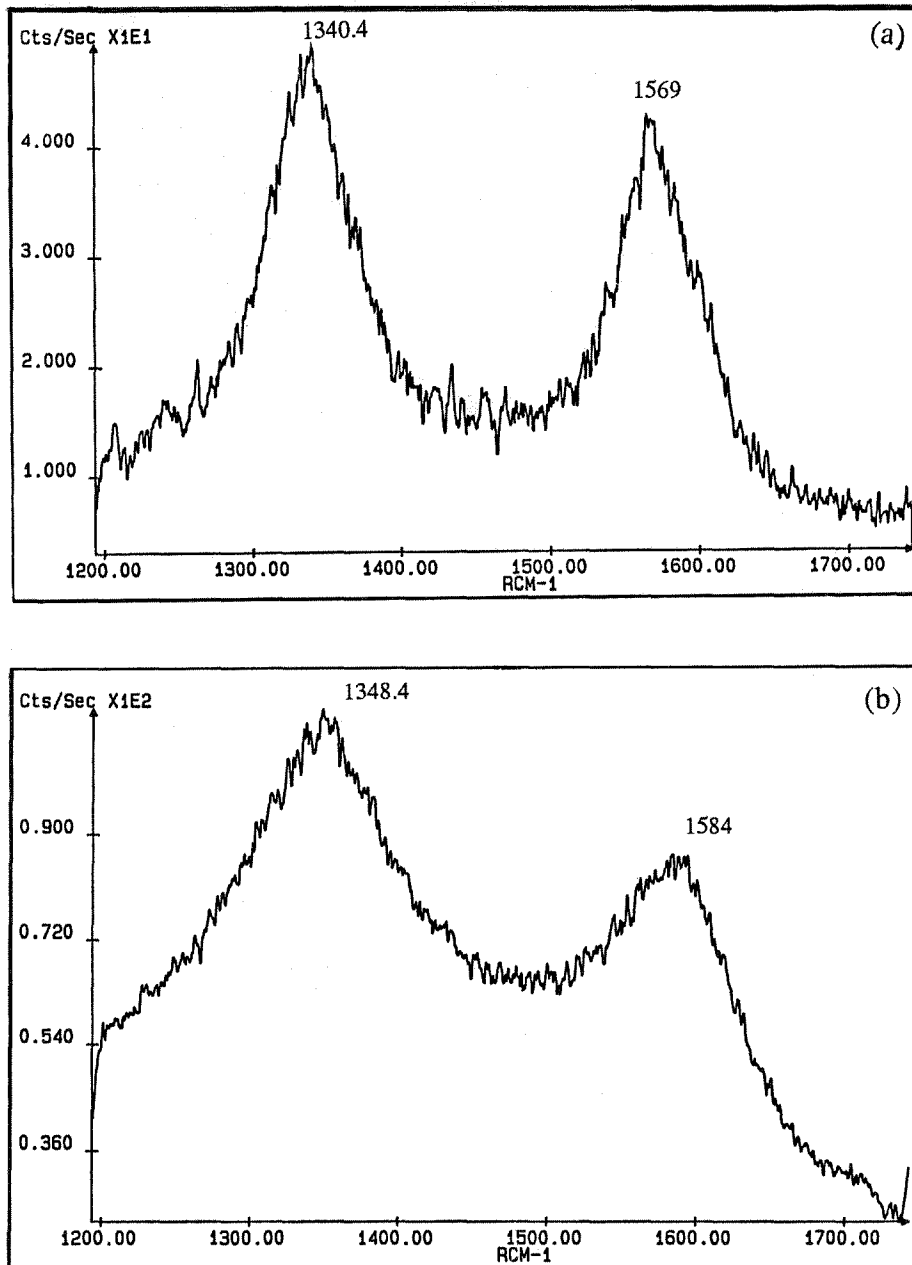


Fig. 7 Raman spectra of the carbon deposits, (a) deposit in Fig. 3, (b) deposit in Fig. 2

The surface morphology of the deposits depends on the laser irradiance and the gas pressure. This was studied by scanning electron microscopy (SEM). Fig. 8 shows the surfaces of carbon rods which were grown with $P_{\text{tot}} = 10\text{W}$, $p_{\text{C}_2\text{H}_2} = 200\text{ Torr}$ (Fig. 8a) and $P_{\text{tot}} = 5\text{W}$, $p_{\text{C}_2\text{H}_2} = 200\text{ Torr}$ (Fig. 8b). At low laser power, the deposition is kinetically limited and relatively uniform deposition profiles are obtained (Fig. 8b). When the reactor is operated in the mass transport limited region, where the rate determining step is the diffusion of the reactant gases to the substrate or deposited film surface, the ball-like particles with size of about $10\mu\text{m}$ are obtained (Fig. 8a).

The carbon rings adhered not so strongly on the alumina substrate.

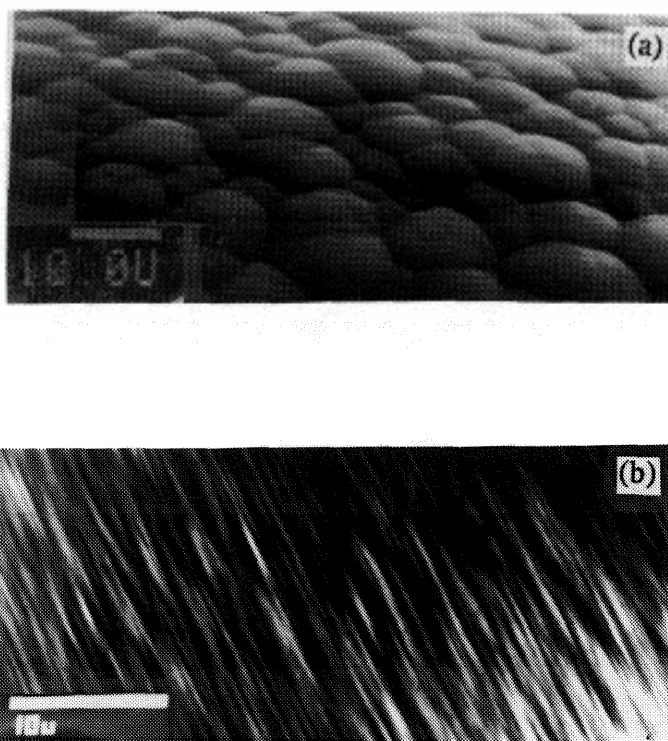


Fig. 8 Surface morphology of carbon deposits at (a) $P_{\text{tot}} = 10\text{W}$, $p_{\text{C}_2\text{H}_2} = 200\text{ Torr}$ and (b) $P_{\text{tot}} = 5\text{W}$, $p_{\text{C}_2\text{H}_2} = 200\text{ Torr}$.

4.SUMMARY

In summary, a selective area laser deposition system has been built to perform solid freeform fabrication from gas phase. The initial results show a promising future of the new technique.

Acknowledgements

The authors wish to express their gratitude to Diane Armellino and Fran Adar of Instruments SA, Inc. for the Raman spectra measurements. The assistance of Norman Williams and Don Artieschoufsky in the design and fabrication of the system is gratefully acknowledged. This research was supported by a Texas Advanced Research project.

References

1. C. Arnone, M. Rothschild, J. G. Black, and D. J. Ehrlich, *Appl. Phys. Lett.* **48**, 14 (1986).
2. T. T. Kodas, T. H. Baum, and P. B. Comita, *J. Appl. Phys.* **62**, 281 (1987).
3. H. L. Marcus, J. J. Beaman, J. W. Barlow, and D. L. Bourell, *Ceramic bulletin*, **69**, 1030 (1990).
4. D. S. Knight and W. B. White, *J. Mater. Res.*, **4**, 385 (1989).
5. L. S. Plano and F. Adar, *SPIE vol. 822 Raman and Luminescence Spectroscopy in Technology*, 52 (1987).